Growth of curved graphene sheets on graphite by chemical vapor deposition

I. Kholmanov,[1,*] E. Cavaliere,[1,2] M. Fanetti,[1,2] C. Cepek,[1] and L. Gavioli[1,2]
[1]*Laboratorio Nazionale, TASC-CNR-INFM, SS 14, Km 163.5, Basovizza, IT-34012 Trieste, Italy*
[2]*Dipartimento di Matematica e Fisica, Università Cattolica del Sacro Cuore, via dei Musei 41, IT-25121 Brescia, Italy*
(Received 22 May 2009; published 15 June 2009)

We report a synthesis route of a carbon-based structure, curved graphene sheet (CGS). The CGS grows by catalytic chemical vapor deposition autoselectively at the stacked bilayer edges of graphite support, providing an atomically smooth connection of the edges. We propose a growth mechanism based on Fe nanoparticle diffusion along the step edges, acting as a nanozipper. The work addresses with a simple experimental method, the edge engineering in graphene bilayer systems. The results may have a significant impact on the fabrication of new carbon nanostructures and their integration into nanoelectronics.

DOI: 10.1103/PhysRevB.79.233403 PACS number(s): 81.07.−b, 61.48.De, 68.37.Ef, 81.15.Gh

Carbon nanostructures play a central role in nanomaterial science and nanotechnology due to the wide diversity of their structural forms and unusual properties. The varieties of carbon forms, such as spheres (fullerenes such as C_{60}), tubes (carbon nanotubes), or planes (graphene), have different behavior in relation to the dimensionality of the system, ranging from zero dimensional (0D) (C_{60}) to two dimensions (2D) (graphene).[1–3] In most cases control over the growth parameters might allow to tailor structure, size distribution, spatial arrangement at the nanometer scale, and diverse physical properties of carbon nanostructures. Development of advanced synthesis methods, therefore, is remaining one of the basic issues of the investigations of carbon nanostructures.

Catalytic chemical vapor deposition (CVD) of hydrocarbon gases is a well-developed and widely used method to produce a certain type of high-quality nanostructured carbon materials with controlled characteristics. Efficiency of this method is determined by the right combination of hydrocarbon gas, catalysts, catalyst supports, reaction pressure, and temperature at which gas decomposition occurs.[2,4–6]

A conceptually different approach to fabricate some types of carbon nanostructures is based on the production of these nanostructures directly from graphite. In particular, single graphene layers[3] have been produced by mechanical exfoliation of graphite. Additionally, the first multiwall carbon nanotubes (MWCNTs) were proposed to be formed by the folding of graphite sheet followed by sheet sealing during the electric arc process.[7] Recently, Yu and Liu[8] theoretically demonstrated the synthesis of single-wall carbon nanotubes (SWCNTs) by rolling up the graphene sheets through adsorption of hydrogen and fluorine gases on the sheet that can induce the surface stress driving the sheet-to-tube transition. However, the practical realization of the CNT production by direct sheet-to-nanotube transformation is not yet achieved. Instead, experimental investigations of a possible graphene-nanotube transformation have stimulated the synthesis and study of new carbon nanostructures, such as scrolls,[9,10] foldings,[11] ripples,[12] and sleeves[13] that share some common features of carbon nanotubes and graphene sheets.

In this work, we report a synthesis route of a carbon-based structure, namely, curved graphene sheet (CGS), that is an intermediate structure between a carbon nanotube and a flat graphene sheet. Moreover, we propose a zipping growth mechanism and discuss the origin of the CGS shape. Our idea is based on the combination of the above-described methods (CVD and graphite-based procedures), namely, we synthesize the CGS by CVD of methane on highly oriented pyrolytic graphite (HOPG) at relatively low temperatures using Fe catalytic nanoparticles. This approach exploits the weak film-substrate interaction[14] and the edge decoration of HOPG support by Fe nanoparticles,[15] achieving the localization of the CVD growth process at the HOPG step edges. Scanning tunneling microscopy (STM) data show that the CGS have grown at the edges of graphite double steps, connecting the edges of two stacked layers.

The HOPG specimen (ZYB grade, 3×5 mm^2), used in our experiments, has been cleaved in air and immediately inserted in the experimental chamber of a multiscan OMICRON STM/SEM/SAM ultrahigh vacuum (UHV) system (base pressure of about 5×10^{-11} mbar), where it has been thoroughly degassed up to 900 °C for 30 min. All further experiments, including Fe deposition and CVD of methane described below, have been performed *in situ*. All the STM images presented in this work have been obtained in constant current mode at room temperature and reported z values have been calibrated measuring single, double, and triple steps of HOPG. Part of the STM data analysis has been performed with WSXM software.[16] Fe deposition on HOPG has been performed with the substrate at room temperature using a high-voltage *e*-beam sublimator. A fixed Fe deposition rate of ~0.8 Å/min, measured by a quartz oscillator, has been obtained by keeping constant the evaporation power at ~3.0 W (emission current on the Fe rod: 4.2–5 mA, voltage applied to the Fe rod: 600–700 V). The CVD process has been done by using methane (99.99% pure) as precursor gas at a pressure inside the experimental chamber at 2×10^{-4} mbar.

Atomically flat (0001) basal planes and step edges of different height can be produced by simple cleaving the HOPG at ambient conditions. Deposition of Fe on this substrate results in the growth of three-dimensional (3D) metal nanoparticles by Volmer-Weber mode, as observed for most transition-metal films on HOPG support.[14,15] At low coverage the Fe nanoparticles preferentially decorate the step edges of topmost graphene layers, while the HOPG terraces remain almost completely uncovered [Fig. 1(a)]. The metal nanoparticles remain at the step edges even after the anneal-

 ©2009 The American Physical Society

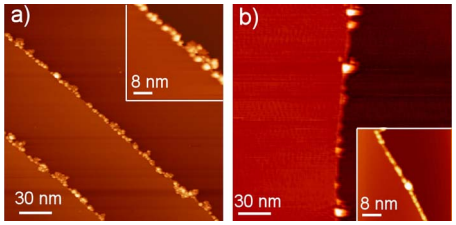

FIG. 1. (Color online) STM images (200×200 nm^2) of HOPG support with step edges decorated by catalytic Fe nanoparticles: (a) as-deposited ($V=-2.0$ V, $I=0.2$ nA) and (b) after annealing at 900 °C without methane in UHV conditions ($V=-1.5$ V, $I=0.2$ nA). Insets are higher magnification (40×40 nm^2) of the corresponding STM images. The thermal treatment without methane does not alter the HOPG step edges.

ing treatment in UHV at 900 °C (the temperature used in our experiments for CVD of methane) [Fig. 1(b)]. However, this treatment causes no modifications in the step edges and terraces of the HOPG support.

We exposed the as-deposited Fe nanoparticles shown in Fig. 1(a) to pure methane gas for 3 min, keeping the sample at 900 °C. After this CVD process, the STM data [Fig. 2(a)] show that the terraces of (0001) basal plane of HOPG remains unaffected, while substantial changes are observed at the step edges. In particular, as for the annealing without methane [Fig. 1(b)], the number of metal nanoparticles trapped at the step edges is significantly decreased, indicating the Fe re-evaporation from the HOPG substrate during the CVD process. The most intriguing observation is however the presence of curved structures grown along the step edges [Figs. 2(a) and 2(b)], that we name CGS, with the principal axis shown as dotted lines in Fig. 2(a). This observation indicates the localization of CVD reaction at steps due to their decoration by metal catalysts. Calibrated constant current profile analysis of STM images [green (upper) curve of inset plot in Fig. 2(a)] shows that the height of the step edges, along which the CGSs are located, is 0.68 ± 0.04 nm, which is very close to double graphene step height (0.671

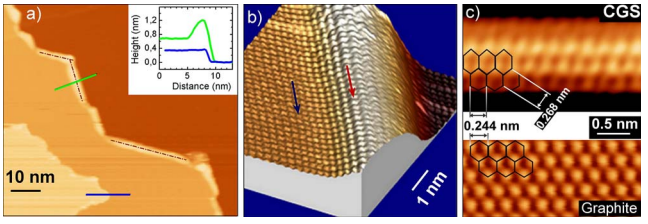

FIG. 2. (Color online) The Fe/HOPG system after CVD process and the grown CGS. (a) STM image (79×72 nm^2) ($V=+1.5$ V, $I=0.5$ nA) of Fe/HOPG containing topmost single and double planes, with several CGSs grown only at double step edges. Dot-dashed lines indicate the CGS principal axis. Constant current profiles, taken across single (blue horizontal line) and double (green line) steps, are plotted in the inset. (b) Atomically resolved STM image ($V=+0.02$ V, $I=0.031$ nA) of a CGS in 3D view. The CGS principal axis (red arrow) has same direction with lattice vector of graphene (blue arrow). (c) Atomically resolved STM images of CGS (upper panel) and graphite (lower panel) ($V=+0.3$ V, $I=0.5$ nA).

nm). It is important to note that no CGS has been observed at the edges of single steps [blue curve of inset plot in Fig. 2(a)]. Moreover, to verify that the CGS growth actually takes place only when the Fe catalyst is present at the step edges, we exposed to methane the clean HOPG support without Fe particles at the same growth conditions for CVD. This treatment leads to the formation of amorphous carbon at the step edges.

The atomically resolved STM image displayed in 3D view [Fig. 2(b)] shows that one lateral side of the CGS (left side in the image) is continuously connected to the terrace of the topmost graphite plane. This observation clearly exhibits the difference of CGS from the SWCNTs since the latter is a closed cylindrical structure. In addition, the atomic resolution, allowing observing the honeycomb lattice at both sides of the CGS, is lost when the CGS is curving down toward the bottom plane [right side of the CGS shown in Fig. 2(b)]. This is likely due to the tip curvature radius, since the total height of the structure with respect to the bottom plane in Fig. 2(b) is about 1.2 nm. Therefore electrons from the CGS will tunnel into the tip side when the tip is moving toward or away from the CGS, but it still over the bottom plane. This hampers the possibility to observe the actual shape of this side of CGS.

Remarkably, the lattice vector of the CGS, oriented along the principal axis [red arrow in Fig. 2(b)], is running parallel to the vector direction of the graphene crystal lattice [dark blue arrow in Fig. 2(b)]. Therefore, the apparent structure of the CGS is morphologically very similar to graphene foldings.[11] However, some features of the CGS make it clearly different from folded planes. In particular, a single folding of a graphene sheet produces only one bended structure (similar to CGS) with one principal axis and one folded part of the sheet as a topmost plane.[11] In contrast, the STM image presented in Fig. 2(a) shows a single topmost plane surrounded by several adjacent CGS with the principal axis (dash-dotted line) oriented in different directions. Moreover, we do not observe any folded plane behind the CGS. Thus, it is clear that the CGS is not a folded plane and cannot be produced by folding the graphene sheet.

The atomically resolved STM image of CGS [upper image in Fig. 2(c)] displays honeycomb structure similar to the STM image of SWCNT.[17,18] This is clearly different from the STM images of (0001) HOPG planes [lower image in Fig. 2(c)], where the usual threefold symmetry corresponding to the intensity maxima only three (β atoms) of the six carbon atoms of the honeycomb lattice are observed.[19] However, along the CGS axis the distance between two nearest β carbon atoms is 0.245 ± 0.008 nm, which is equal to the corresponding value in graphite [0.24 ± 0.008 nm (Ref. 19)]. In contrast, perpendicular to the CGS axis, the corresponding distance is about 9% larger (0.268 ± 0.008 nm), demonstrating a lattice distortion (angles and bond length) induced by the CGS curvature. This behavior is similar to the theoretically suggested distortion for carbon nanotubes.[20] The overall apparent view fits with distorted hexagons, as shown in Fig. 2(c). The CGS atomic structure also suggests a similarity of the curved structure with armchair SWCNT that would have the axis parallel to the CGS axis. Note also that the angle between the principal axes of two different CGS is

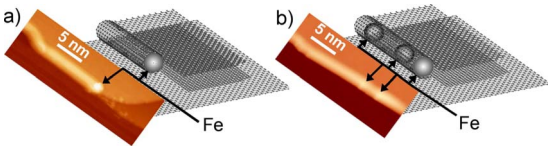

FIG. 3. (Color online) STM data and corresponding schematic view based on the proposed growth mechanism. (a) (10×32 nm^2) STM image of a CGS with one Fe nanoparticle at one end and related scheme. (b) (10×27 nm^2) STM image of a CGS with few Fe nanoparticles inside and related scheme. The Fe particles are indicated by arrows. The schemes are not to scale with data.

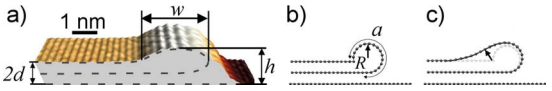

FIG. 4. (Color online) (a) STM image of CGS in 3D view to highlight the structure profile. Dashed lines mark graphene planes and the CGS shape. $\boldsymbol{d}$ is the HOPG plane spacing, $\boldsymbol{w}$ is the CGS width, and $\boldsymbol{h}$ is the height measured with respect to the bottom plane. (b) Schematic model to evaluate the CGS strain energy, assuming a circular CGS curvature, as for a CNT. $\boldsymbol{a}$ is the CGS arc length and $\boldsymbol{R}$ is the curvature radius. (c) Schematic model to mimic the release of the CGS strain energy at the contact point between CGS and graphene plane. The schemes are not to scale with data.

120° [Fig. 2(a)], corresponding to the threefold crystalline symmetry of the graphite cell. This implies that any CGS would have the same "chirality vector," being a structure grown between two stacked edges with same termination.

We have observed that CGS ends where two graphite edges diverge from each other [Fig. 3(a)]. In addition, the Fe nanoparticles have been observed in various parts of the CGS, namely, at its ends [Fig. 3(a)] and/or inside the CGS, far from the extremities [Fig. 3(b)]. To interpret these observations we propose a growth mechanism taking into account the step decoration features of Fe catalysts on HOPG substrate and the dynamical modification of catalyst particles recently suggested.[5] Fe particles trapped at the topmost graphite edges act as catalysts, where the decomposition of methane molecules can take place. The initial stage of CGS growth develops with a mechanism similar to the catalytic CVD growth of CNT, namely, carbon dissolves into the catalyst and CNTs grow by precipitation of excess carbon on the metal surface or carbon may diffuse over the surface particle and feed the CNT structure.[5,21] Over the surface of the catalyst particle, the carbon atoms from fragmented CH_4 can meet the graphite edges in contact with the Fe particle and create chemical bonds with the edge atoms. In case of graphite double steps with trapped Fe particles, this mechanism takes place on both graphene layers and the growing structure follows the metal particle curvature, forming by this way a curved structure, joining the two stacked planes, and eliminating the abruptly terminated edges. Such a direct way to engineer the system at the atomic scale represents a very promising approach that goes beyond the possibilities of lithographic techniques. Furthermore, the diffusion of the metal particle along the step edge during the CVD process allows the growth of the curved structure along the entire step, hence creating the CGS by a zipperlike mechanism (slide fastener). In this case the Fe particles can be found only at the one end of the CGS [Fig. 3(a)]. This resembles the "top" growth mode of CNT.[22] Additionally, given the concentration of Fe particles at the step edges, it is likely that during the CVD reaction a Fe particle, diffusing along the step edges, may meet another one. This leads to the situation in which one of the Fe particles remains trapped inside the CGS, while the other continues the growth processes. This can explain the numerous observations of the CGS with a Fe particle trapped inside them [Fig. 3(b)]. The described growth mechanism requires that the catalyst metal particle be in contact with the edges of both stacked graphene planes in order to obtain a CGS. This is consistent with the experimental data showing that the CGS growth stops when the Fe particle reaches a location where the two stacked plane edges diverge [Fig. 3(a)]. One should note that the temperature required for the CGS growth might lower depending on the precursor gas as for CNT synthesis.[1,5] We expect that the use of C_2H_2 could decrease the growth temperature down to around 500 °C.

STM image in Fig. 4(a) illustrates a cross-sectional 3D view of the CGS. The dimensions measured experimentally are width $\boldsymbol{w}=2.1\pm0.05$ nm and height $\boldsymbol{h}=1.15\pm0.08$ nm, measured with respect to the bottom plane. The experimental errors are obtained considering tip convolution effects, possible electronic contributions to the tip z displacement, and the tunneling conditions. The height of the CGS [Fig. 3(a)] is obtained by supposing that the CGS bottom part should not be in contact with the underlying graphite plane, but would keep the (0001) graphite plane spacing, i.e., $\boldsymbol{d}=0.34$ nm, due to the van der Waals repulsion. Therefore, $\boldsymbol{h}_{CGS}=\boldsymbol{h}-\boldsymbol{d}=0.81\pm0.08$ nm, that in combination with $\boldsymbol{w}$ indicates a quasielliptical shape of the CGS structure. These values are in good agreement with the corresponding values of folded graphene sheet that we produced by the STM tip (images not shown).

The quasielliptical shape of CGS can be explained by considering the relaxation of curvature-induced strain energy of CGS in the contact with planar graphene bilayer that initially has no strain energy. To estimate the CGS strain energy per unit area we approximate the experimentally observed quasielliptic shape with a circular shape [Fig. 4(b)] and we employ the curvature-induced strain energy as for CNT,[11,23] $E_{CGS}=(kal)/R^2$, where $k=1.4$ eV is the curvature modulus for carbon nanotubes, a, l, and R are the arc length, the length of CGS, and the radius of curvature, respectively [Fig. 4(b)]. The energy per unit area is obtained from $E_{CGS}/(al)=8.33$ eV/nm^2 for a unit length of 1 nm and $R=0.41$ nm. The planar graphene sheets, on the other hand, are characterized by an attractive interlayer van der Waals energy E_{vdW}, which can be determined by $E_{vdW}=-\varepsilon_{vdW}S$, where $\varepsilon_{vdW}=2$ eV/nm^2 and S is the surface area.[11] Therefore the calculated energy per unit surface area in the CGS is about 4 times larger than the van der Waals energy existing between planar graphene sheets. The excess strain energy is released, eliminating the kink by lifting up a part of the topmost planar graphene sheet near contact region [Fig. 4(c)], thus forming a smoothed shape and resulting in the experimentally observed

quasielliptic shape. We note that CGS is not an isolated structure such as carbon nanotubes, where a definite relation between the diameter of CNT and the catalytic particle size exists.[1,5] Here, the correlation between CGS and Fe particle size is limited by graphene bilayer interactions. The final diameter and shape of the CGS are mainly determined by the energy relaxation of the growing CGS+graphene bilayer system. Hence the CGS diameter dependence on the Fe particle size is likely a secondary effect.

In summary, we report for the first time the edge engineering in graphene bilayer systems by a simple method allowing the control of the edge structures at the atomic scale. The new synthesis route allows controlling the growth of the CGS that occurs autoselectively at the stacked bilayer edges of graphite support. Since CGS is a morphological intermediate between CNT and planar graphene, such nanostructures could potentially have different physical properties. One of the important characteristics of this structure is the elimination of edge structures that could modify the edge effects on the electronic properties of the system. Application of our method can lead to formation of new nanostructures, such as graphene bilayer quantum dots or antidots with edges closed through CGS. Moreover, our method might also be applied to other graphene bilayer systems, for instance, to graphene bilayers grown on SiC by thermal sublimation. Finally, graphene bilayers with CGS-terminated edges can be considered as a promising material for hydrogen storage systems or magnetic storage elements.

This work has been partially funded by "FIRB Carbon-based microstructures and nanostructures" and by the "PRIN2006" programs of MIUR.

*On leave from Heat Physics Department, Academy of Sciences, Uzbekistan.

[1] M. Knupfer, Surf. Sci. Rep. **42**, 1 (2001).
[2] H. Dai, Surf. Sci. **500**, 218 (2002).
[3] K. S. Novoselov, A. K. Geim, S. V. Morozov, D. Jiang, M. I. Katsnelson, I. V. Grigorieva, S. V. Dubonos, and A. A. Firsov, Nature (London) **438**, 197 (2005).
[4] A. Reina, X. Jia, J. Ho, D. Nezich, H. Son, V. Bulovic, M. S. Dresselhaus, and J. Kong, Nano Lett. **9**, 30 (2009).
[5] S. Hofmann, R. Sharma, C. Ducati, G. Du, C. Mattevi, C. Cepek, M. Cantoro, S. Pisana, A. Parvez, F. Cervantes-Sodi, A. C. Ferrari, R. Dunin-Borkowski, S. Lizzit, L. Petaccia, A. Goldoni, and J. Robertson, Nano Lett. **7**, 602 (2007).
[6] T. de los Arcos, F. Vonau, M. G. Garnier, V. Thommen, H.-G. Boyen, P. Oelhafen, M. Düggelin, D. Mathis, and R. Guggenheim, Appl. Phys. Lett. **80**, 2383 (2002).
[7] S. Iijima, Nature (London) **354**, 56 (1991).
[8] D. Yu and F. Liu, Nano Lett. **7**, 3046 (2007).
[9] S. Berber and D. Tománek, Phys. Rev. B **69**, 233404 (2004).
[10] J. G. Lavin, S. Subramoney, R. S. Ruoff, S. Berber, and D. Tománek, Carbon **40**, 1123 (2002).
[11] H. V. Roy, C. Kallinger, and K. Sattler, Surf. Sci. **407**, 1 (1998).
[12] H. Hiura, W. Ebbesen, J. Fujita, K. Tanigaki, and T. Takada, Nature (London) **367**, 148 (1994).
[13] S. V. Rotkin and Y. Gogotsi, Mater. Res. Innovations **5**, 191 (2002).
[14] C. Binns, S. H. Baker, C. Demangeat, and J. C. Parlebas, Surf. Sci. Rep. **34**, 107 (1999).
[15] I. N. Kholmanov, L. Gavioli, M. Fanetti, M. Casella, C. Cepek, C. Mattevi, and M. Sancrotti, Surf. Sci. **601**, 188 (2007).
[16] I. Horcas, R. Fernández, J. M. Gómez-Rodríguez, and J. Colchero, Rev. Sci. Instrum. **78**, 013705 (2007).
[17] J. W. G. Wilder, L. C. Venema, A. G. Rinzler, R. E. Smalley, and C. Dekker, Nature (London) **391**, 59 (1998).
[18] T. W. Odom, J.-L. Huang, Ph. Kim, and Ch. M. Lieber, Nature (London) **391**, 62 (1998).
[19] S. Hembacher, F. J. Giessibl, J. Mannhart, and C. F. Quate, Phys. Rev. Lett. **94**, 056101 (2005).
[20] O. Gülseren, T. Yildirim, and S. Ciraci, Phys. Rev. B **65**, 153405 (2002).
[21] J. Gavillet, A. Loiseau, C. Journet, F. Willaime, F. Ducastelle, and J. C. Charlier, Phys. Rev. Lett. **87**, 275504 (2001).
[22] H. Dai, A. G. Rinzler, P. Nikolaev, A. Thess, D. T. Colbert, and R. E. Smalley, Chem. Phys. Lett. **260**, 471 (1996).
[23] N. G. Chopra, L. X. Benedict, V. H. Crespi, M. L. Cohen, S. G. Louie, and A. Zettl, Nature (London) **377**, 135 (1995).